Original Article

An approach for the calculation of characteristics I – V and P – V curves in BIPV arrays

Una aproximación para el cálculo de las curvas características I – V y P – V en arreglos BIPV

Luz Adriana Trejos Grisales[1]

[1] Escuela de Ingeniería Electromecánica, Facultad Seccional Duitama, Universidad Pedagógica y Tecnológica de Colombia, Duitama, Boyacá, Colombia.

Abstract

Objective: The main objective of this work is to obtain a procedure based on mathematical and geometry relationships to calculate the radiation and shadows effect in vertical surfaces and obtain profiles for analyzing BIPV arrays installed on the vertical surface in terms of the I –V and P – V curves.

Methodology: The proposed approach has three stages. The first is oriented to the study of Sun behavior in order to calculate the required information for estimating the radiation components for vertical surfaces. The second stage is oriented to analyze the effect of shadows of object in the neighborhood of the vertical surface. The third stage is oriented to the calculation of the I –V and P – V curves of a BIPV array.

Results: An approach for the calculation the radiation behavior and shadow analysis for vertical surfaces in the context of BIPV solutions was developed to obtain the I –V and P – V curves of a BIPV array. The solution was implemented in Matlab® but it can be extended to other platforms for a more generalized used.

Conclusions: The proposed solution allowed to obtain the I –V and P – V curves of a study case BIPV array based on the radiation and shadow analysis of the vertical surface. Results were compared with simulation in BIMsolar software. The percentage of area affected by shading calculated by using the proposed solution differs 1.9 % from BIMsolar results

Keywords: BIPV array, vertical surface, radiation components, shadow, PV array curves.

Resumen

Objetivo: El objetivo principal de este trabajo es obtener un procedimiento basado en relaciones matemáticas y geométricas para calcular la radiación y el efecto de las sombras en superficies verticales y obtener perfiles para analizar arreglos BIPV instalados en dichas superficies en términos de las curvas I – V y P – V.

Metodología: El enfoque propuesto consta de tres etapas. La primera se centra en el estudio del comportamiento solar para calcular la información necesaria para estimar los componentes de radiación en superficies verticales. La segunda se centra en el análisis del efecto de las sombras de los objetos cercanos a la superficie vertical. La tercera en el cálculo de las curvas I – V y P – V de un arreglo BIPV.

Resultados: Se desarrolló un método para el cálculo del comportamiento de la radiación y el análisis de sombras en superficies verticales, en el contexto de soluciones BIPV, con el fin de obtener las curvas I – V y P – V de un arreglo BIPV. La solución se implementó en Matlab®, pero puede extenderse a otras plataformas para un uso más generalizado.

Conclusiones: La solución propuesta permitió obtener las curvas I – V y P – V de un arreglo BIPV de estudio, basándose en el análisis de radiación y sombras de la superficie vertical. Los resultados se compararon con una simulación en el software BIMsolar.

Palabras clave: arreglo BIPV, superficie vertical, componentes de radiación, sombra, curvas arreglo PV.

Spanish version

What were the most relevant findings?

The Sun behavior and radiation was characterized through a set of equations; the effect of shadow was represented by performing an analyze of the basic characteristics of an object surrounding the vertical surface under study. The solar parameters such as solar altitude and solar azimuth were compared with the software BIMsolar achieving MAPE values of 15.51 %. The radiation was also estimated with a MAPE of 15.66 %. The procedure was able to obtain the radiation profile to calculate the I − V and P − V curves of a BIPV study case.

What do these findings contribute?

The proposed approach was implemented in Matlab® but can be extended to other platforms. In this way, the solution can be used even in embedded devices for dc-dc converter control purposes. The proposed solution can be the base model for future developments that allow to improve the understanding of BIPV solutions without the requirements of commercial software tools contributing to the development of new solutions in PV systems.

Graphical Abstract
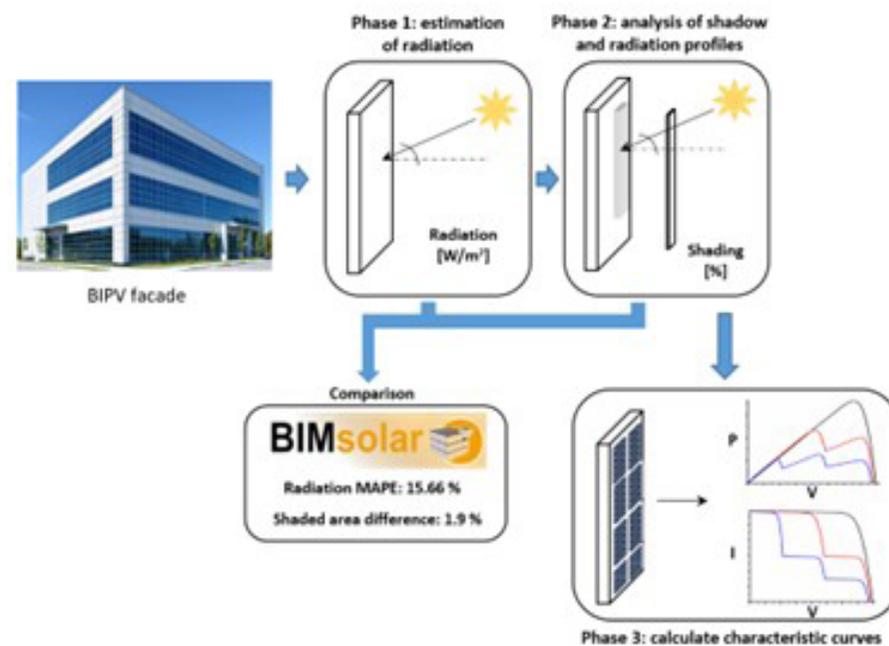
Introduction

Energy generation using solar panels has grown significantly in recent years, consolidating it as a competitive option to face current energy and environmental challenges. Thus, installed renewable energy capacity in 2024 will reach 4443 GW, of which 1866 GW corresponds to solar photovoltaic energy, representing 42 % of the global renewable energy mix. This value, in turn, represents 19 % of the global energy mix, including non-renewable sources (1).

Due to current advances in materials and other devices associated with electricity generation in photovoltaic systems, photovoltaic applications are no longer limited to the installation of panels on roofs and open fields (solar farms). Building integrated photovoltaic (BIPV) systems are becoming as one of the most interesting applications today due to their high potential for use in urban environments where demand is constantly increasing. These systems use photovoltaic modules or panels as active structural components of buildings, for example: facades, windows, corridor ceilings, balconies, among others. They generally focus on utilizing structural surfaces that may be exposed to solar radiation while maintaining consistency with architectural requirements (2). Figure 1 shows some of the parts of a building structure which can be used in BIPV solutions.

Figure 1. (1) Roof, (2) PV rain curtain, (3) PV sun shield, (4) PV skylight, (5) PV facade, (6) PV wall. Adopted from (3).

According to (4) BIPV solutions have developed most strongly in Europe. In particular, Italy reports the largest installed capacity for this type of system, with more than 2.5 GW; this has largely been leveraged by the tariff schemes implemented by the country's government, which are attractive to users. Other countries such as the Netherlands, Austria, and Australia have reported installed capacity values between 29 MW and 0.15 GW. In Spain, Sweden, and Finland, values between 0.08 GW and 2.64 GW have been reported. On the other hand, in Asia, particularly in China and Japan, BIPV projects have been developed, especially in the commercial sector, with powers of up to 235 kW (5). At the time of writing this paper, no specific data on installed capacity in the Americas was available. However, it is noteworthy, for example, that a study conducted in Canada in 2006

showed an energy potential of 71.34 TWh that could be generated from BIPV systems in residential, commercial, and institutional buildings. Currently, at least 50 BIPV projects are registered BIPV (6). Meanwhile, in the United States, the development of these types of projects has been encouraged through various strategies by the Department of Energy (DOE) (7) and various stakeholders in the industrial and commercial sectors that promote the benefits of LEED (Leadership in Energy and Environmental Design) certifications, which entail tax breaks and visibility in the field of energy efficiency innovation (8). In the specific case of Latin America, some studies report a growing interest in the topic. Authors in (9) present a study of a BIPV system located in Joao Pessoa, Brazil; simulation and experimental analyses were used to identify a potential annual generation of up to 81.6 kWh. The work of (10) presents a study focused on the energy potential of a building belonging to the Salesian Polytechnic University, located in Guayaquil, Ecuador, considering the use of one of the building's facades as the study area. The analysis performed by simulation allowed to identify a potential annual generation of 6281 kWh.

One of the important aspects in PV applications in general is the identification of radiation profiles which allow to evaluate the power potential given an array structure of topology. In BIPV applications this is also an important matter since the position of PV elements will differ from the conventional applications; surfaces such as facades, walls and windows are placed perpendicular to the horizontal plane. On the other hand, partial shading may affect the energy generation. In fact, BIPV systems could be more susceptible to this condition since the aforementioned orientation of the PV elements which could be exposed to shadowing from other buildings, chimneys, poles, among others. In general, partial shading condition is widespread in urban areas which is the main spotlight of application of BIPV solutions (11), (12). In this way, the calculation of accurate radiation profiles would provide suitable estimation of P-V (power vs. voltage) characteristics and energy estimations. Different methods have been proposed in the literature to address the calculation of radiation profiles or energy potential in surfaces such as facades. Such methods are usually based on models which represent the behavior or the Sun through equations, or are based in analysis of information provided by tools that integrate 3D characteristics and geographical information. In (13) authors proposed a solution to estimate energy potential in urban facades based on a linear regression model with information provide by GIS (geographic information system) software, Laser imaging, detection, and ranging, or LiDAR and weather databases. The model requires the creation of 3D characteristics of buildings which was performed by using ESRI® ArcGIS software. However, there is no detailed information concerning the procedure for estimating the radiation from weather data which makes the solution difficult to replicate. On the other hand, in (14) transposition models are used to calculate irradiance profiles for vertical surfaces using data of diffuse and global irradiation from PVGIS tool. The models area based in solar geometry equations such as the Perez and Muneer models which defines explicit expressions for calculation of irradiance. Then, authors proposed a combination of the models. The solution is validated with experimental tests which evidenced errors provoked by the complexity of including partial shading effects. In (15) the Perez model is also used to define the characteristics of the behavior of irradiance for estimating PV potential in buildings; the proposed procedure integrates building vector data for creating 3D models and Hillshade analysis tool from ESRI® ArcGIS software, the Ladybug tool is also used for analyzing partial shading effects. The work presented in (16) provides

an analysis on the optimal orientation of vertical surfaces for PV harvesting by using a set of equation to represent the behavior of the sun and the irradiance components along with the Python PVLib package and data from National Solar Radiation Database (NSRDB). Three study cases are presented in different cities of Colombia which allowed to evidence the influence of the location; partial shading effects are not included in the analysis.

On the other hand, the use of computing tools or software to simulate BIPV systems have been reported in several works; in (17) an assessment model for facades in BIPV systems is proposed. The authors proposed the use of a BIM (Building Information Modeling) framework integrating Rhino for the 3D structure aspects and Grasshopper and Ladybug for photovoltaic analysis. The model is used for analyzing a study case located in Taiwan and it provides not only results concerning energy aspects but also economic evaluation. In (18) facades are studied too in terms of the possible location of panels for a study case in Saudi Arabia by using the commercial software PVsyst which allows to identify that the best location provides the 68% of the energy demand of the building. On the other hand, the work reported in (19) proposed the use on neural networks for developing a digital twin to model a BIPV system for facades located in Madrid to predict the generated power; the model allows to include the impact of shadowing due to other buildings. The model presented relative errors from 6% to 15% in comparison with actual measurements. In (12) authors used Simulink for analyzing partial shading effects in roofs and facades for BIPV systems including the study of configurations such as TCT (total-cross-tied); radiation information was taken from data bases, however, authors did not specify which one was used or the location of the study case. The prediction of the annual energy potential in BIPV systems is addressed in (20); the study was performed for climate conditions of 15 cities in China. The prediction was made by using Rhino for 3D modeling and EnergyPlus for energy calculations; the results allowed to identify the different potential of the locations given primary useful data for future BIPV projects. In (21) EnergyPlus was also used for the study of office buildings in China; the details concerning the including method of radiation data was not given. However, the results were compared with experimental test, which allowed to identify suitable BIPV strategies for the implementation of projects integrating roof and sun shade devices. Finally, the work presented in (22) presented a comparison of 8 software tools applied to an actual study case located in China. The work presented an exhaustive form the results obtained by each software tool and the comparison between them in terms of the predicted energy. Authors considered popular and commercial software tools such as PV*SOL, PVsyst and SAM and others oriented to building modeling such as BIMsolar; one of the main results of this work is the identification of advantages and drawbacks of the tools which allows to the user selecting the proper tool depending on the analysis needs.

From the literature review it was identified that estimation and assessment of radiation profiles is an active research topic in which tools such as PVGIS, ArcGIS, solar geometry models have been reported and also there is the possibility of using software tools as reported in (17) to (22). However, the mentioned tools are supported by medium and high complexity levels of development or require purchasing a software tool. On the other hand, the analysis of P - V curves for analyzing the shading impact is not fully addressed neither for power estimation nor for developing of control strategies for maximum power point tracking. Therefore, this paper introduces an approach for the

calculation of power in BIPV arrays based on a procedure for calculating radiation profiles based on solar geometry equations combined with a technique for modeling PV arrays which allows to simulate the BIPV array for obtaining the P-V curves. The procedure admits the use of some objects which can describe in a general way the neighborhood of the BIPV array and cause shades. The procedure proposed in this work is implemented in Matlab® but can be replicated by using other computing languages, this providing the opportunity of using the algorithms in other computing platforms or even in embedded devices for dc-dc converter control purposes. The paper is organized as follows: section 2 is dedicated to describe the mathematical procedures for estimating the radiation and the shadow analysis for a vertical surface. Section 3 presents the study case for validate the proposed approach. Section 4 is devoted to the results and discussion and section 5 presents the conclusions of the work.

Materials and methods

This work proposes as methodology phases, the following: (i) estimation of radiation in a vertical surface given its area, latitude, longitude and other parameters correspond to time of the year; (ii) analysis of objects or structures in the neighborhood of the vertical surface that can project shadows for calculation of the radiation profile; (iii) calculation of characteristic curves for an array in which the area of the vertical surface defines the number of panels and its possible configuration. Figure 2 illustrate the proposed procedure.
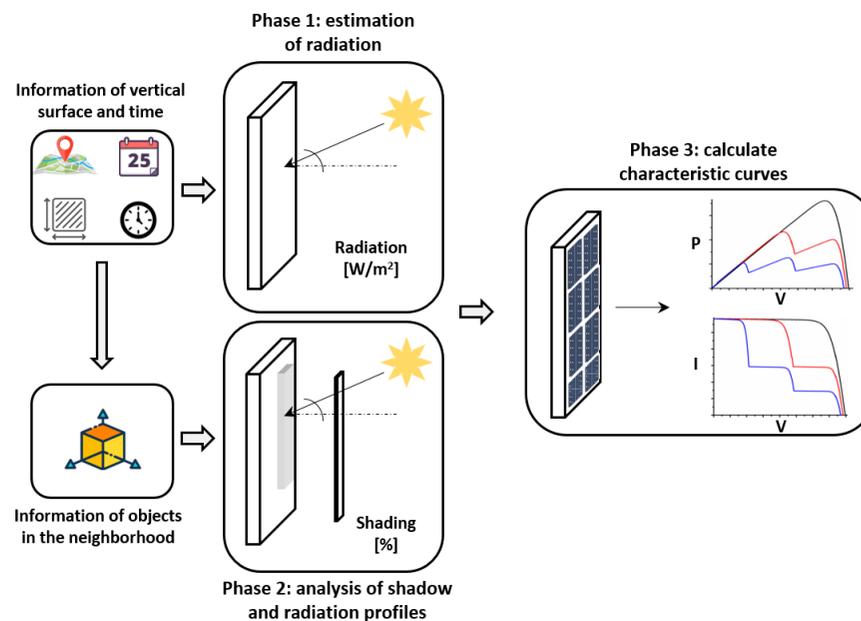

Figure 2. Methodology proposed in this work.

Solar geometry relationships for radiation estimation

To study the behavior of radiation and shades in a given location and considering attributes such as height, width and position of any structure it is required to consider the fundamental equations of solar geometry which describe the Sun behavior. The procedures described in the following are based on (23) which in turn describes the model proposed by Iqbal which is widely accepted for solar calculations in engineering. The declination angle δ gives the angular position of the sun at solar noon with respect to the equator, it can be calculated using 1 with N representing the day of the year under study.

$$\delta = 23.45 * \sin\left(360 * \frac{(284 + N)}{365}\right) \tag{1}$$

To stablish the correct relationships in solar geometry it is required to calculate the solar time S_t which differs from the local clock time L_t since it is based on the apparent angular motion of the sun across its trajectory. The expression of 2 is used to calculate the solar time, with E being the term related with the correction in minutes for the day under study; the equations for calculating E are giving in 3 and 4; M_{st} and M_{loc} correspond to the standard meridian for the local time zone and the longitude of the location under analysis, respectively.

$$S_t = L_t + 4 * (M_{st} - M_{loc}) + E \tag{2}$$

$$E = 229.2 * (0.000075 + 0.001868 * \cos B - 0.032077 * \sin B - 0.014615 * \cos 2B \\ - 0.04089 * \sin B) \tag{3}$$

$$B = 360 * \frac{N - 1}{365} \tag{4}$$

Finally, the angular displacement of the sun east or west of the local meridian due its own rotation is giving by the hour angle ω expressed in 5, which is useful to represent the Sun position in the sky considering horizontal and vertical planes.

$$\omega = 15 * (S_t - 12) \tag{5}$$

Figure 3, shows the angles and components which describe the Sun position. The solar altitude angle α can be calculated through exploring the geometry relationships and the information concerning the day and time; as expressed in (23) equation 6 provides a practical form to obtain the solar altitude where ϕ is the latitude. In this way, from the calculation of α it is possible to identify that for values lower than 0° the sun is below the horizon giving no shadow.

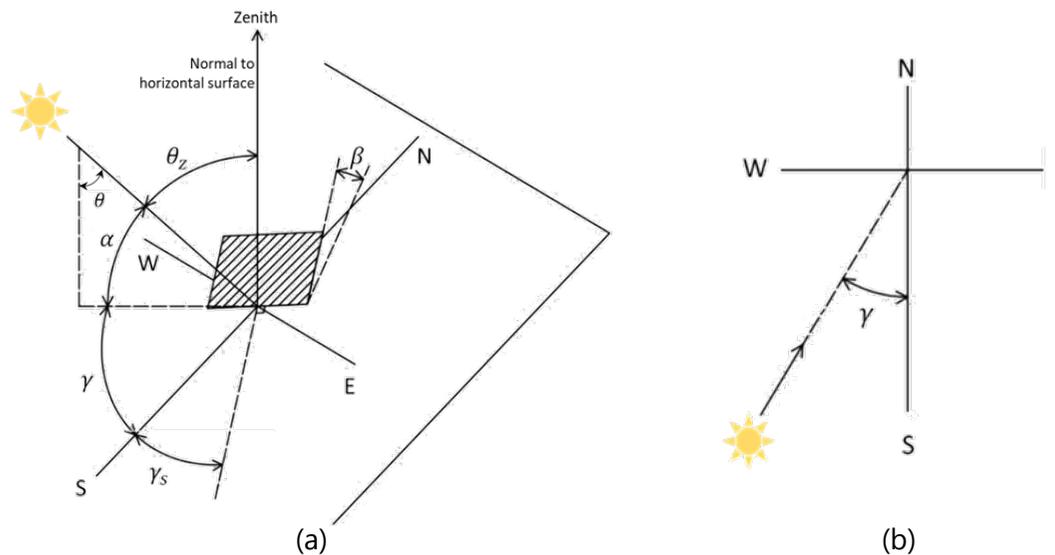**Figure 3.** (a) angles and components which describe the Sun position. (b) Top view for azimuth angle.

On the other hand, the solar azimuth angle γ which is expressed by equations 7 to 9, helps to identify the behavior of the projection of beam radiation on the horizontal plane. Finally 10 represents the incidence angle θ which depends on γ and the surface azimuth γ_s, this considering that for vertical surfaces the slope β is 90°. It allows to define if Sun is behind or in front of the surface.

$$\alpha = \sin^{-1}(\sin\phi * \sin\delta + \cos\phi * \cos\delta * \cos\omega) \tag{6}$$

$$\sin\gamma = \frac{\cos\delta * \sin\omega}{\cos\alpha} \tag{7}$$

$$\cos\gamma = \frac{\sin\delta * \cos\phi - \cos\delta * \sin\phi * \cos\omega}{\cos\alpha} \tag{8}$$

$$\gamma = \tan^{-1}(\sin\gamma, \cos\gamma) \tag{9}$$

$$\theta = \gamma - \gamma_s \tag{10}$$

The components of radiation which allow to estimate the radiation on the surface under study are the direct horizontal radiation and the diffuse horizontal radiation defined as G_b and G_d respectively in this work. Once the position of the Sun is defined for a given moment and day, the components of the radiation can be defined. First, the extraterrestrial radiation is obtained by applying 11 with G_{sc} = 1367 W/m²; then, to consider the effect of the atmosphere it is necessary to calculate de total beam transmittance τ_b defined in 12, in which τ_R corresponds with the Rayleigh transmittance which considers the fixed air mass m_f that takes into account the altitude of the location under study; τ_a corresponds with the transmittance due to the aerosols presence where A_β and m are the Angstrom beta parameter and the air mass, respectively. τ_g corresponds with the transmittance of aerosols; τ_w corresponds with the water vapor transmittance (23). In this work equations 13 to 16 were used to calculate the factors mentioned before in order to represent realistic conditions. In 12 the fixed air mass m_f is calculated as $m * (P/P_0)$, with P and P_0 corresponding with the atmospheric pressure at the altitude of the location under study and the atmospheric pressure at sea level, respectively. The air mass m corresponds to $1/\cos(\theta_z)$, where θ_z is the complementary angle of

the solar altitude angle α. In addition, considering that A_β varies from 0 to 0.4, for very clean to very turbid atmospheres respectively (23), in this work a value of 0.1 was considered to represent an average condition.

$$G_{on} = G_{sc} * (1.000110 + 0.034221 * \cos B + 0.001280 * \sin B + 0.00719 * \cos 2B + 0.000077 * \sin 2B) \tag{11}$$

$$\tau_b = \tau_R * \tau_a * \tau_g * \tau_w \tag{12}$$

$$\tau_R = e^{\left(-0.0903*m_f^{0.84}*\left(1+m_f-m_f^{1.01}\right)\right)} \tag{13}$$

$$\tau_a = e^{-A_\beta^{0.873}*\left(1+A_\beta^{0.873}-A_\beta^{0.7088}\right)*m^{0.9108}} \tag{14}$$

$$\tau_g = e^{\left(-0.0127*m^{0.26}\right)} \tag{15}$$

$$\tau_w = e^{\left(-0.477*m/(1+40.14*m)^{0.45}\right)} \tag{16}$$

Finally, G_b and G_d are defined by 17 and 18. In addition, in this work the albedo component, which corresponds to the measurement of the fraction of the global horizontal irradiation that is reflected from the ground, was considered by assuming a ground reflectance of 0.2 (23). In this way, equation 19 provides the calculation for the albedo component. The sum of the three components is equivalent to the total radiation G_t as expressed in 20.

$$G_b = G_{on} * \tau_b * (\cos \theta / \sin \alpha) \tag{17}$$

$$G_d = G_{on} * 0.5 * (1 - \tau_R * \tau_a) * (1 - \tau_b) \tag{18}$$

$$A = 0.2 * (G_{on} * \tau_b + G_d) \tag{19}$$

$$G_t = G_b + G_d + A \tag{20}$$

Analysis of objects surrounding the study surface

To evaluate the possible shade effects from objects in the neighborhood of the vertical surface under study, it is necessary to define the main attributes of the system. In this work height (H_v) and width (W_v) are used to define the vertical surface; while height (H_o), width (W_o), depth (D_o) and position (X_o, Y_o) are used to define the objects in the neighborhood of the vertical surface. The position is defined by assuming the origin of the plane is the half of H_v. In particular, in this section the case of one object will be described; however, the procedure can be extended to more objects. Figure 4 and 5 show how the vertical surface and the objects in the neighborhood are characterized from a top view and a lateral view, respectively. The figures represent the case in which the vertical surface under study corresponds with H_v = 6 m and W_v = 8 m. Object 1 represents a billboard advertising with H_{o1} = 4 m, W_{o1} = 4 m and D_{o1} = 1 m, while object 2 represents a small building with H_{o2} = 6 m, W_{o2} = 6 m and D_{o2} = 4 m.
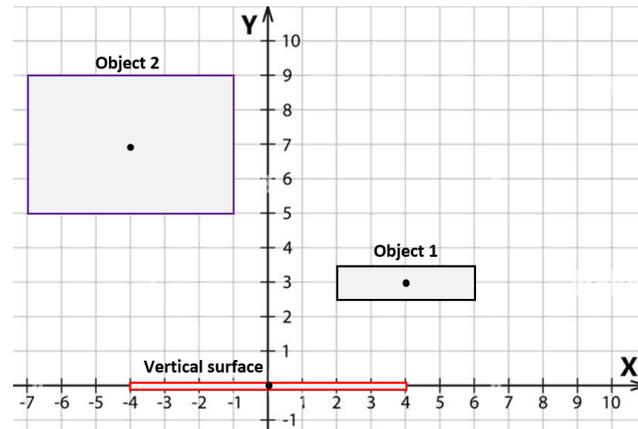
Figure 4. Characterization of vertical surface and the objects in the neighborhood from top view.
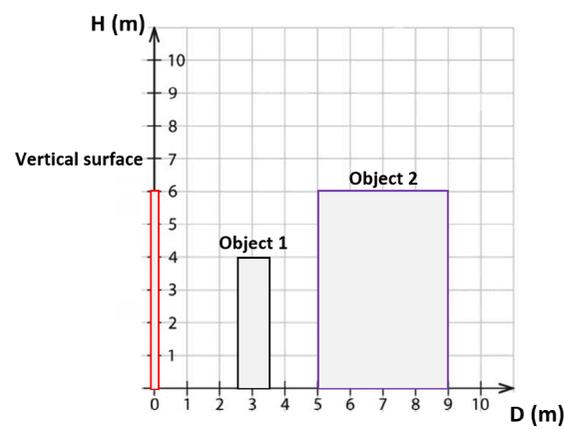

Figure 5. Characterization of vertical surface and the objects in the neighborhood from lateral view.

Object 1 begins at 2.5 m in front to the vertical surface, then that information is taken as reference to place the object considering its dimensions; in this case X_{o1} = 4 m and Y_{o1} = 3 m. If the same is applied to object 2 then X_{o2} = -4 m and Y_{o2} = 7 m. In this way, an object can be defined by a matrix such the one presented in 21. The sub index i represents the number of the object. The matrix must have as many rows as objects want to be studied.

$$Obj = [H_{oi}, W_{oi}, D_{oi}, X_{oi}, Y_{oi}] \tag{21}$$

The horizontal shadow longitude L_{hs} is expressed in 22, from which some restrictions will apply for α. From the relationships given by the position of the components of the system under analysis, equations 23 and 24 describe the information require to describe the direction of the shadow. In this way, the direction of the shadow can be identified in order to verify if there is influence on the vertical surface under study. With C_x and C_y corresponding with the coordinates of the corners of the object, the position of shadow can be defined by 25 and 26.

$$L_{hs} = H_o / \tan \alpha \tag{22}$$
$$D_x = L_{hs} * \sin \gamma \tag{23}$$
$$D_y = -L_{hs} * \cos \gamma \tag{24}$$
$$S_{x\,(1\times4)} = [C_x]_{(1\times4)} + D_x \tag{25}$$

$$S_{y\,(1\times4)} = \left[C_y\right]_{(1\times4)} + D_y \tag{26}$$

From equations 25 and 26 it must be defined if the shadow of the corners intercepts the surface, this by performing a comparison with the position of the surface on the plane in terms of the Y axis ($S_y < 0$). In order to analyze the behavior of shadow when it crosses the horizontal axis, an interception parameter is defined in 27; it allows to calculate the position of the shadow with respect the surface in the X axis by using 28 and the height of the shadow by using 29. If P_{sz} is lower than 0 it means that the shadow of the corner does not reach the surface. Figure 6 illustrates the considered relationships.

$$I_{(1\times4)} = \left[C_y\right]_{1\times4} / \left(\left[C_y\right]_{1\times4} - S_y\right) \tag{27}$$
$$P_{sx\,(1\times4)} = \left[C_x\right]_{1\times4} + I * \left(S_x - \left[C_x\right]_{1\times4}\right) \tag{28}$$
$$P_{sz\,(1\times4)} = H_o - I * L_{hs} * \tan\alpha \tag{29}$$
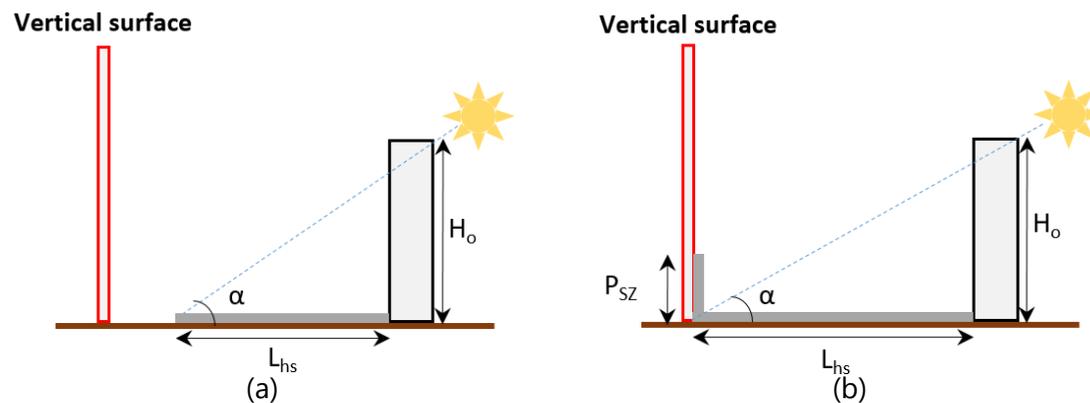

Figure 6. (a) Shadow does not reach the vertical surface ($S_y > 0$). (b) Shadow of corners reaches the vertical surface and it projects on the surface ($S_y < 0$ and $P_{sz} > 0$).

When all four corners of the object are analyzed and it is confirmed that the object projects a shadow on the vertical surface, its dimensions must be calculated and then compared in terms of the area with the surface under study to define the percentage of shaded area. For that purpose, the limits of the shadow with respect to the width of the vertical surface must be defined. Figure 7 illustrates the information that must be considered in order to calculate the shadow limits, taking as reference the case of object 1 in Figure 4 for a given Sun behavior described in the study case section.
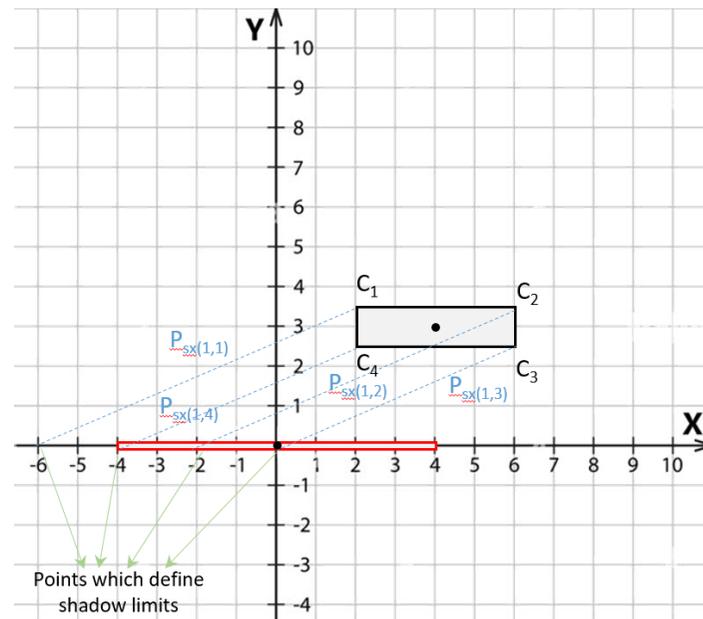
Figure 7. Position of the shadow projected by corners of object with respect to X axis.

Once the limits of the shadow are identified, it is possible to calculate the area of the shadow by calculating its effective width (E_w) with respect to the vertical surface width and the maximum of P_{sz}. Figure 8 presents a rear view of the case illustrated in Figure 7 in which it is observed the parameters to consider for the calculation of the shadow area (A_{sh}) as expressed in 30.
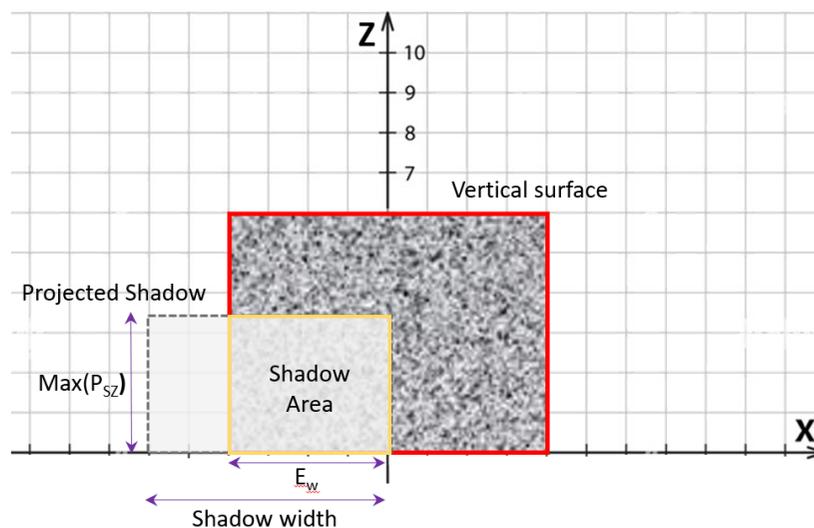

Figure 8. Rear view of vertical surface and shadow with the parameters to calculate the shadow area.

$$A_{sh} = max(P_{sz}) * E_w \tag{30}$$

Finally, to obtain the irradiance profile of the vertical surface, it is required to know the dimensions of photovoltaic elements covering the vertical surface. In this paper the dimensions of a

conventional PV panel are taken as example to illustrate the proposed procedure for obtaining the irradiance profile. The PV panels characteristics were obtained from the BIMsolar software database, which is the tool used for validating the proposed procedure. In this way, the BIMsolar 340 W, 1100 mm X 1980 mm PV panel was used; considering the dimensions of the vertical surface (H_v = 6 m and W_v = 8 m), an array of 3 x 7 panels can be set as facade. In consequence, the irradiance profile P_G will be defined as a 3 x 7 matrix in which each element represents the irradiance available for each PV panel. By using simulations based on reported works to study the behavior of panels under partial shading conditions at cell level (24), it was identified how to define the impact of shadow in terms of the affected area in the panel; therefore, if the affected area is greater than 60%, the panel will be considered fully shaded. Figure 9 presents a front view of the reference case in which it is observed how the panels of the second row at right are affected significantly. According to the defined criterion those panels will be considered fully shaded. Moreover, since the object considered in this work has a solid surface which means that it is not made of translucent material, the shadow will completely block the irradiance. By applying the procedure described for the radiation estimation, the irradiance profile matrix for the reference case in this study can be expressed by 31.
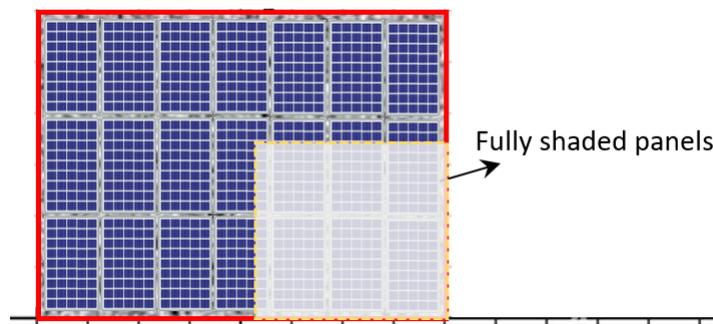

Figure 9. Front view of vertical surface with panels and projected shadow.

$$P_G = \begin{bmatrix} G_t & G_t & G_t & G_t & G_t & G_t & G_t \\ G_t & G_t & G_t & G_t & 0 & 0 & 0 \\ G_t & G_t & G_t & G_t & 0 & 0 & 0 \end{bmatrix} \tag{31}$$

Figure 10 presents the flowchart of the proposed procedure for the calculation of the irradiance profile in vertical surfaces. In the flowchart it is considered that more than one object will be studied. In that case, the total shadow area will be the contribution of all the shadow areas of each object with respect to the vertical surface area. Finally, the resultant irradiance profile will be the input for the algorithm which calculates the characteristic curves I- V and P- V explained in the next section.
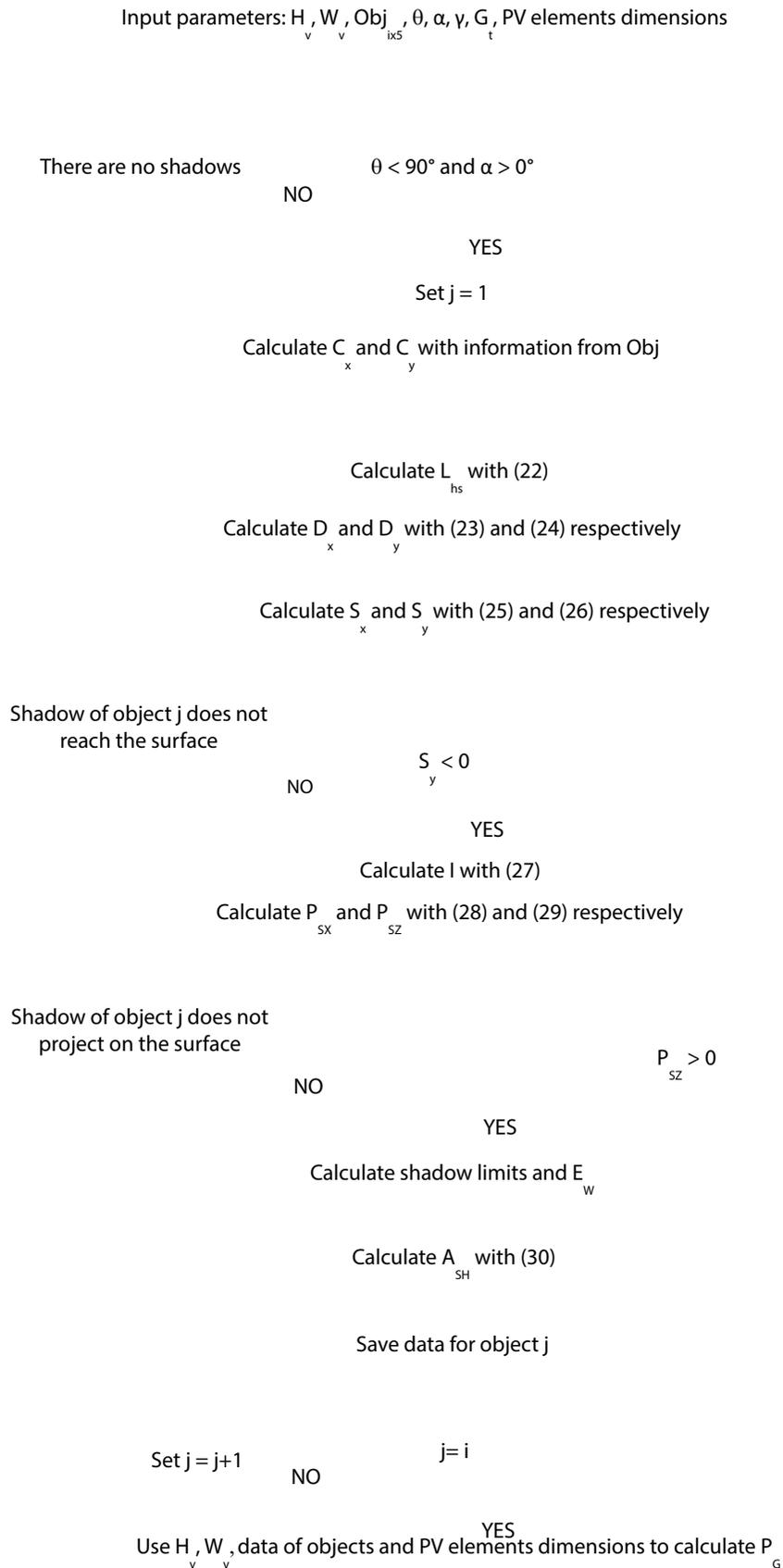
Input parameters: H_v, W_v, Obj_{ix5}, θ, α, γ, G_t, PV elements dimensions

There are no shadows $\qquad$ $\theta < 90°$ and $\alpha > 0°$

NO

YES

Set j = 1

Calculate C_x and C_y with information from Obj

Calculate L_{hs} with (22)

Calculate D_x and D_y with (23) and (24) respectively

Calculate S_x and S_y with (25) and (26) respectively

Shadow of object j does not reach the surface $\qquad$ $S_y < 0$

NO

YES

Calculate I with (27)

Calculate P_{sx} and P_{sz} with (28) and (29) respectively

Shadow of object j does not project on the surface $\qquad$ $P_{sz} > 0$

NO

YES

Calculate shadow limits and E_w

Calculate A_{SH} with (30)

Save data for object j

Set j = j+1 $\qquad$ j= i

NO

YES

Use H_v, W_v, data of objects and PV elements dimensions to calculate P_G

Figure 10. Flowchart of the proposed procedure for the calculation of the irradiance profile in vertical surfaces.

P- V curves analysis

The technique for modeling PV arrays reported in (25) was adopted in this work to evaluate the obtained radiation profiles and obtaining the P-V curves of the BIPV array. The model used for representing the PV cell was the single diode model which is widely accepted thanks to its good compromise between complexity and accuracy. The circuit of the model is shown in Figure 11.
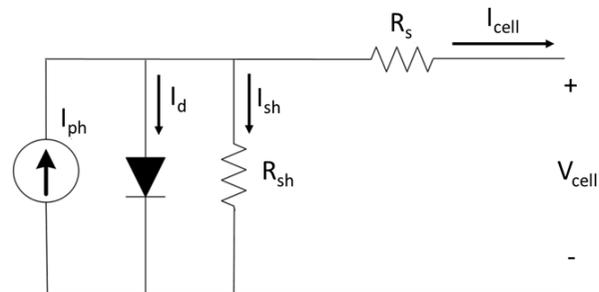

Figure 11. Single diode model of a PV cell.

From the circuit, the equation that represents the relationship between the voltage and current of the cell is presented in 32, where I_{ph} is the photovoltaic current, I_{sat} the saturation current of the diode which represents the semiconductor material, R_s and R_{sh} the resistance associated to the losses and n the ideality factor. Finally, Vt is known as the thermal voltage $V_t = kT/q$, with k equal to the Bolztmann constant, T the cell temperature in Kelvin and q the charge of an electron.

$$I_{cell} = I_{ph} - I_{sat}\left(e^{((V_{cell} + I_{cell} * R_s)/n * V_t)} - 1\right) - \frac{(V_{cell} + I_{cell} * R_s)}{R_{sh}} \tag{32}$$

Due to the strong non-linear relationship between the voltage and current of the cell, the work presented in (25) uses the Lambert W function which allows to perform a voltage sweep to calculate the current for a given radiation profile. The modeling procedure considers a PV module as the minimum unit for the analysis, thus the bypass diode of the module must be also considered through its saturation current I_{sat_bd} and thermal voltage V_{t_bd}. Then, the following information to analyze the I-V and P-V curves of an array is required: parameters of the PV modules from datasheet (I_{sc}, V_{oc}, I_{mpp}, V_{mpp}, T_{coeff}, N_s) which correspond with the short circuit current, the open circuit voltage, the current and voltage at the maximum power point, the current and voltage temperature coefficients and the number of cells, respectively; the connection of the PV array is also required, it must be included in terms of a 1/0 matrix, in which 1 means that there is a connection between two consecutive strings and 0 means the opposite. The irradiance profile P_G, is the output of the procedure described in Figure 10. On the other hand, the connection matrix is fundamental for the procedure since it allows to define the sub-arrays in which the array is divided to ease its circuital analysis. A sub-array is defined as a part with no links between strings; this is exploited by the modeling procedure since the sub-array can be analyzed as any circuit through the Kirchhoff current (KCL) and voltage (KVL) laws and also by solving the one diode model equations for each module. In this way, after each sub-array is analyzed in terms of a voltage sweep

which depends on the open circuit voltage of the string, the current of the array will correspond with the sum of all the currents of the sub-arrays. More details can be consulted in reference (25). This methodology allows to evaluate different array connections, i.e. series-parallel (SP), total-cross-tied (TCT), bridge-linked (BL), among others, which could be useful in BIPV applications in order to find the best configuration since the high sensitivity of such PV applications to partial shading. The flowchart presented in Figure 12 illustrate the modeling procedure to obtain the characteristic curves. This modeling procedure can be implemented in any programming language in which Lambert W function and packages for solving non-linear equations can be implemented, this resulting in an attractive solution to avoid purchasing simulation tools.
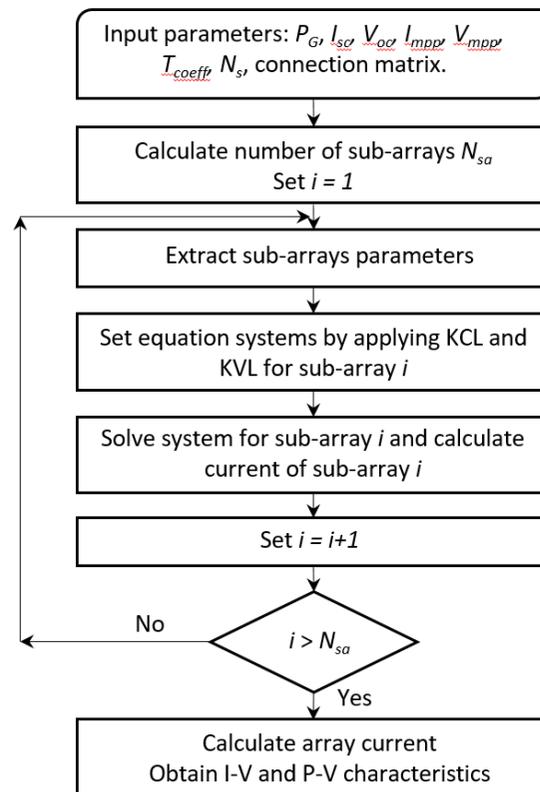

Figure 12. Flowchart of the procedure for obtaining the characteristics curves of a PV array presented in (25).

Study case

In order to validate the proposed procedure, the same case taken as reference in the analysis of shadows section was considered. As it was described, such a case can represent the facade of a building surrounded by a billboard advertising. The dimensions and position are the same already described. Figure 13 (a) and (b) illustrates the conditions of the study case; the figure was designed in SketchUp software using objects available from the software database. On the other hand, Figure 13 (c) and (d) show the representation in terms of the proposed procedure in order to define the parameters required for the shading analysis. The study was performed for all days of July because from simulations performed in BIMsolar it was identified that the radiation for that month was more significant than the current date, considering the position and conditions of the vertical surface.
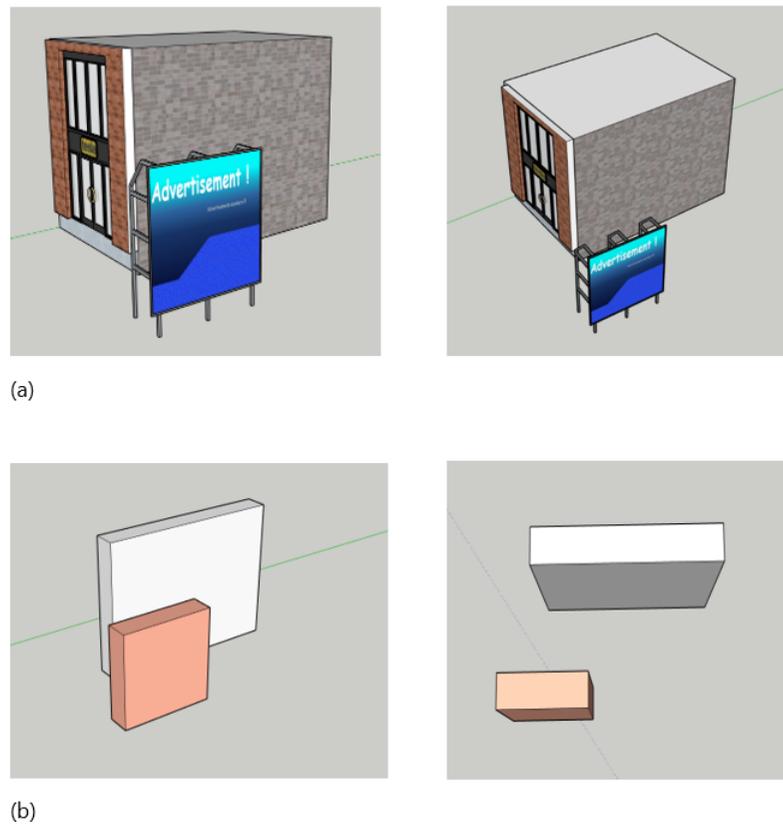
(a)

(b)

Figure 13. (a) Side view of study case structure. (b) Representation of study case in terms of the proposed procedure.

The location of the study case was set in Duitama (Boyacá, Colombia). In terms of the inputs required by the procedure it corresponds with latitude of 5.8269 and a longitude of -73.0331. The city is located at 2590 meters above sea level and the information concerning the time, as it was previously described. The dimensions of the surface under study are H_v = 6 m, W_v = 8 m, and the object information matrix is Obj_{1x5} = [4, 4, 1, 4, 3]. The vertical surface faces north ($\gamma_s = 0°$ for the proposed procedure). The components which describe the Sun behavior were calculated according the solar geometry relationships previously described.

As it was previously informed, the software BIMsolar was used to validate the obtained results in terms of the estimated shadow and radiation behavior. This software tool is oriented to the study of BIPV systems through a platform which requires the 3D model of the structure and its neighborhood, but such a model cannot be implemented in the software; instead must be developed in tools such SketchUp. The software license price is € 690; in this work the trial version of the software was used, such a version has some limitations with respect to capabilities for saving changes in the projects; however, the software allows to obtain the information for performing analysis concerning the radiation components, the solar geometry variables, the power and energy generated, among others. Once the 3D model is set, the user must implement the PV array on the surface under study which implies the user to select the PV module that allows to fit an array considering the dimensions of the surface under study. The next step is to set the connection of

the array and the power interface (DC/DC converter + DC/AC inverter) which in turns defines the configuration of the array, it means, the connection of the modules (SP, TCT, BL), since BIMsolar provides different commercial power interfaces that have requirements in voltage and current. Finally, the software allows to simulate the performance of the BIPV system for a whole year hour by hour. The simulations results include power and energy generated by the BIPV system under study, radiation components values, solar geometry variable values, among others. BIMsolar allows to export the simulation results in Excel files. In this work such option was used to obtain the simulation results from the software in order to compare them with the results obtained with the proposed procedure.

Figure 14 (a) shows the study case implemented in BIMsolar by using the SketchUp model and the settings concerning the location, date and time of the study case. On the other hand, Figure 14 (b) shows the representation in Matlab® of the study case by using the proposed procedure.
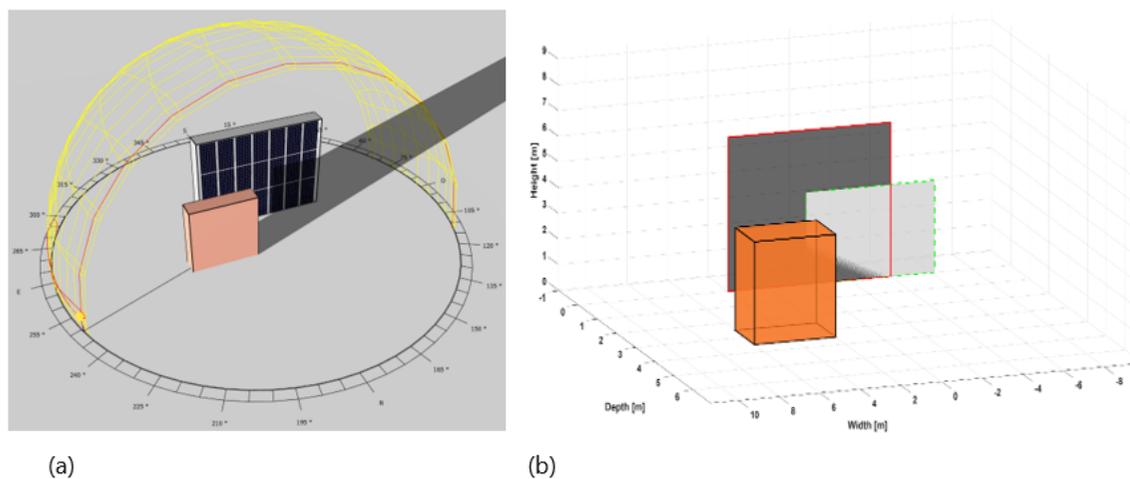

(a)   (b)

Figure 14. (a) Study case implemented in BIMsolar. (b) Representation of the study case in Matlab® using results from the proposed procedure.

Results and Discussion

Figure 15 shows the results of the simulation with BIMsolar in terms of shading proportion in which it is observed that the affected area is 33 %. The percentage of the shaded area obtained by applying the proposed procedure, considering that H_v = 6 m, W_v = 8 m, and A_{sh} = 14.93 m² is 31.1%. Such value corresponds to a difference of 1.9 % with respect to the value obtained with BIMsolar.
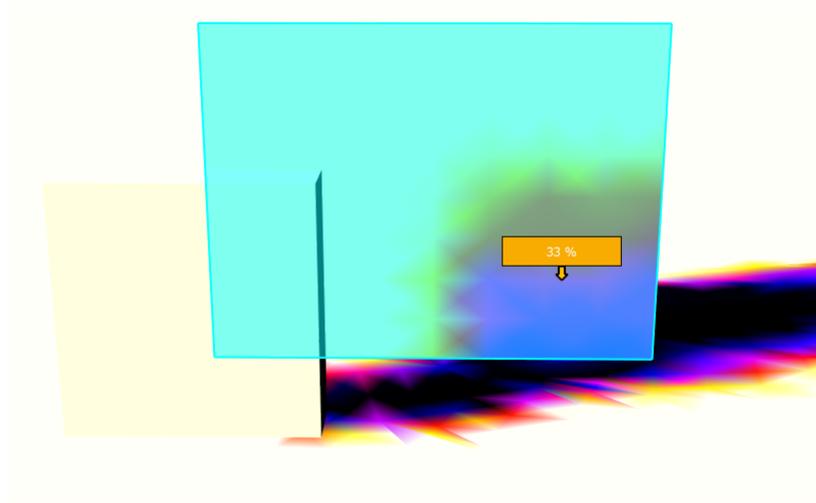
Figure 15. Area affected by shading in BIMsolar.

As stated before, the software BIMsolar allows to export data from simulations included the solar geometry variable values such as solar azimuth and the solar altitude angles, as well as the radiation components hour by hour for one year. For comparison purposes, from the simulations executed in BIMsolar, the information corresponding to July was extracted and then compared with the results provided by the proposed procedure. In this way, the period of time selected for the validation corresponds with the hour 4345 to 5088 of the year. Figure 16, presents the comparison of the solar altitude α; Figure 17 presents the comparison of the solar azimuth γ and Figure 18 presents the components of the radiation. The results were compared in terms of the mean absolute percentage error (MAPE) which are presented in Table 1.
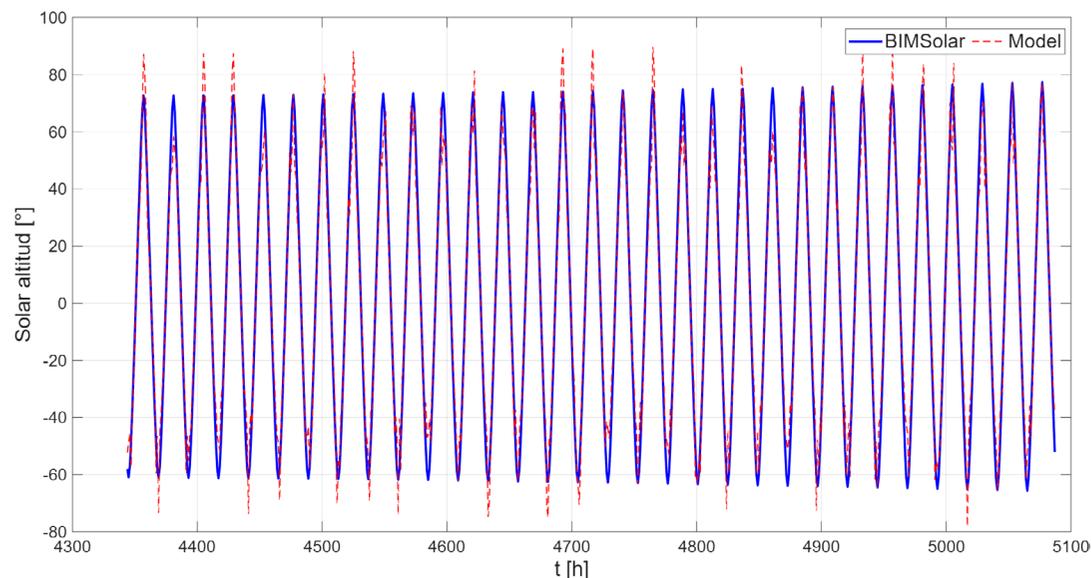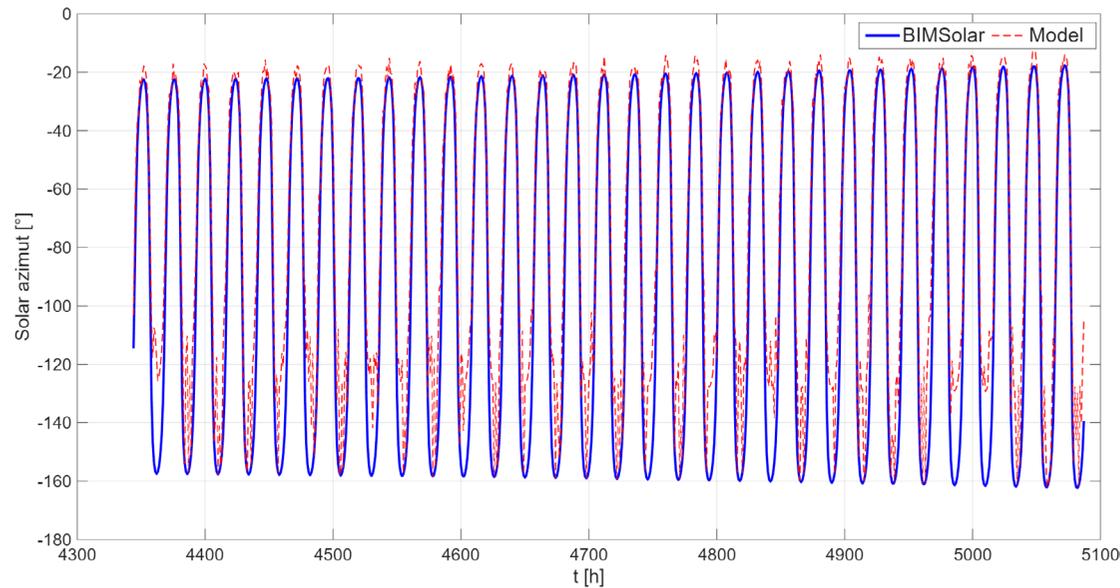

Figure 16. Solar altitude comparison.
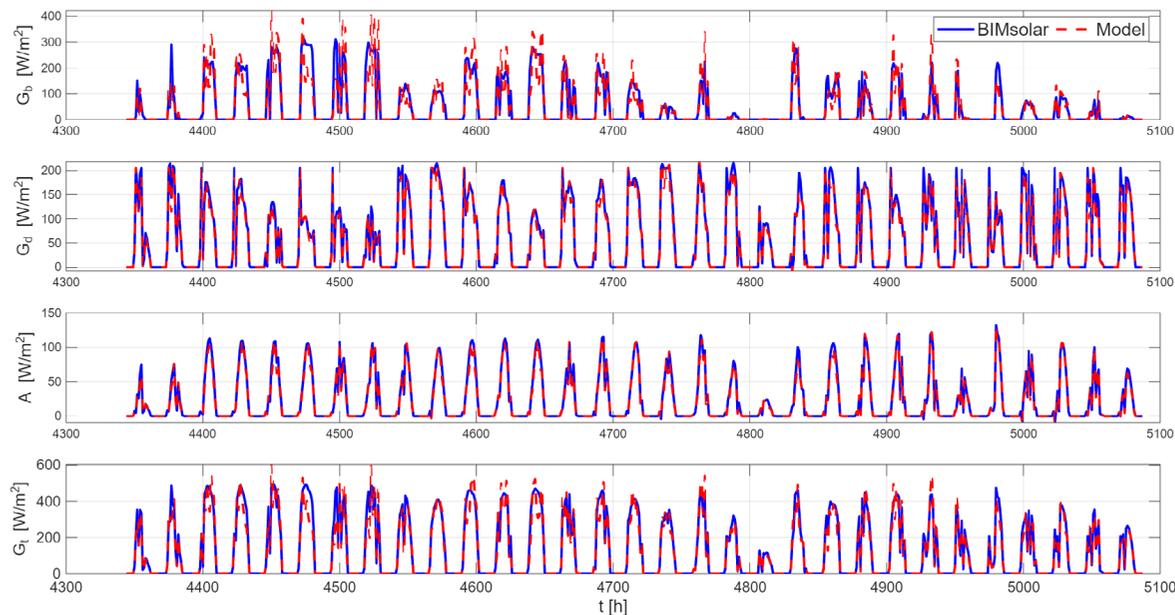
Figure 17. Solar azimuth comparison.

Figure 18. Radiation components comparison.

Table 1. MAPE of variables under comparison

MAPE α	MAPE γ	MAPE G_b	MAPE G_d	MAPE A	MAPE G_t
15.51 %	15.51 %	15.66 %	3.51 %	3.31 %	15.66 %

After the simulations which validated the approaching of the proposed procedure, the characteristic curves analysis was performed. In this way, by applying the procedure described in the flowchart of Figure 10 it was possible to analyze the behavior of the shadow projected on the facade due to the billboard advertising and the irradiance profile was obtained. For a first approach the average value

of G_t for July was adopted; in this way, the irradiance profile matrix obtained is presented in 33.

$$P_G = \begin{bmatrix} 128.72 & 128.72 & 128.72 & 128.72 & 128.72 & 128.72 & 128.72 \\ 128.72 & 128.72 & 128.72 & 128.72 & 0 & 0 & 0 \\ 128.72 & 128.72 & 128.72 & 128.72 & 0 & 0 & 0 \end{bmatrix} \tag{33}$$

With the irradiance profile matrix and the electrical parameters of the PV panel from BIMsolar database presented in table 2, the characteristic curves were obtained by applying the modeling procedure reported in (25). Figure 19 shows the I-V and P-V curves of the PV array considering a SP connection. The maximum power point (MPP) is 479.36 W. If the procedure for obtaining P_G is executed for a defined period of time, the MPPs can be calculated and the average power and energy generation can be estimated.

Table 2. PV panel datasheet parameters.

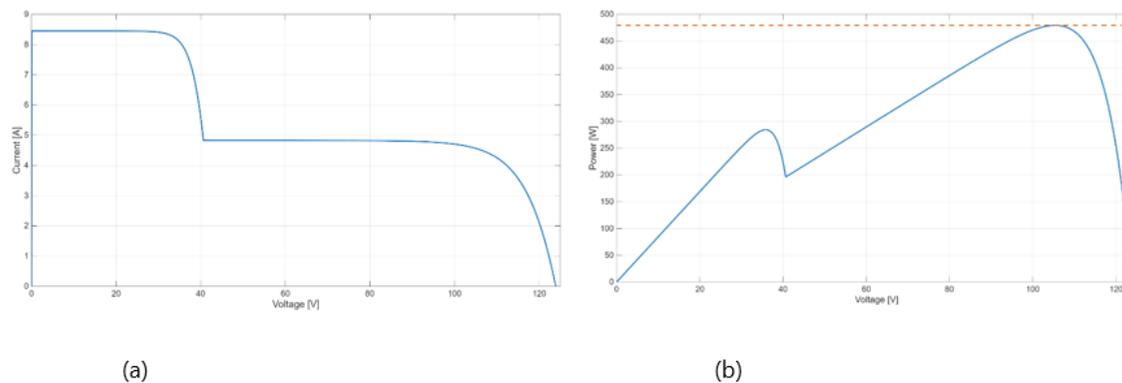| Isc	Voc	Impp	Vmpp	V Tcoeff	I Tcoeff	Ns
9.38 A	46.8 V	8.88 A	38.3 V	-0.32 %/°C	0.05 %/°C	72

(a)

(b)

Figure 19. (a) I-V curve of the PV array on the vertical surface under study. (b) P-V curve of the PV array on the vertical surface under study.

Conclusions

This paper proposed a methodology to estimate the radiation of vertical surfaces and shadow analysis for BIPV applications. The proposed methodology allowed to calculate the radiation components (Beam, diffuse and albedo) for a vertical surface as it was presented through a study case. Results were compared with simulations performed in BIMsolar which is a software currently used for BIPV analysis. The percentage of area affected by shading calculated by using the proposed solution differs 1.9 % from BIMsolar results. On the other hand, the proposed procedure achieved a MAPE of 15.51 % for the solar altitude angle, as well as for the solar azimuth angle. On the other hand, the estimated radiation components exhibited a MAPE of 15.66 %, 3.51 %, 3.31 % and 15.66 % for G_b, G_d, A and G_t, respectively. The relationship of the MAPE value for the angles and G_b is given by the mathematical relationships for their calculation, which are trigonometry relationships that can introduce uncertainties in the final values. In this way, exploring a more detailed geometry expression analysis can reduce the MAPE value; however, it is not clear what is the model used by BIMsolar to calculate the solar angles.

A matrix with the radiation profile per PV panel was obtained and used for calculating the I – V and P – V curve for a study case, achieving the objective of this work. The radiation profile considered the average value of radiation for one month of operation; however, the procedure can be repeated for consecutive radiation profiles (hour by hour) for obtaining the estimation of power and energy for longer periods of time.

The proposed procedure was applied for one object projecting shadow on the vertical surface through geometry relationships, but it can be extended for including more objects and estimate the behavior of radiation and shadow for more complex and realistic scenarios. Moreover, further analysis could consider a detailed evaluation of the effect of shadow in proportion to the affected area to improve the estimation of the irradiance for a panel affected by shadow, this by considering the space that is normally applied to the PV units when are installed.

The proposed approach was implemented in Matlab® but can be replicated by using other computing languages with the functions that guarantee that the mathematical operations of procedures can be performed. In this way, the solution can be used even in embedded devices for dc-dc converter control purposes. Therefore, this approach can be the base model for future developments that allow to improve the understanding of BIPV solutions without the requirements of commercial software tools. In this way, contributing to the development of new solutions in PV systems.

References

1. International Renewable Energy Agency. Renewable energy highlights 2025. [Online].; 2025. Acceso 20 de Agosto de 2025. Disponible en: www.irena.org/-/media/Files/IRENA/Agency/Publication/2025/Jul/IRENA_DAT_Renewable_energy_highlights_2025.pdf

2. Martin-Chivelet N, Kapsis K, Rose Wilson H, Delisle V, Yang R, Olivieri L, et al. Building-Integrated Photovoltaic (BIPV) products and systems: A review of energy-related behavior. Energy and Buildings. 2022;: p. 1-18.

https://doi.org/10.1016/j.enbuild.2022.111998

3. Bosnjakovic M, Katinic M, Cikic A, Muhic S. Building Integrated Photovoltaics Overview of Barriers and Opportunities.Thermal Science. 2023; 27(2B).

https://doi.org/10.2298/TSCI221107030B

4. International Energy Agency. Analysis of Technological Innovation Systems for BIPV in Different IEA Countries. [Online].; 2025. Acceso 15 de Septiembre de 2025. Disponible en: https://iea-pvps.org/key-topics/analysis-of-technological-innovation-systems-for-bipv-in-different-iea-countries/

5. International Energy Agency. Successful Building-integration of Photovoltaics A collection of International Projects. [Online].; 2020. Acceso 15 de Septiembre de 2025. Disponible en: https://iea-pvps.org/key-topics/succesful-building-integration-of-photovoltaics-a-collection-of-international-projects/

6. Natural Resources Canada. Building-integrated Photovoltaics. [Online].; 2025. Acceso 20 de Septiembre de 2025. Disponible en: https://natural-resources.canada.ca/energy-efficiency/building-integrated-photovoltaics

7. Department of Energy. Expanding Solar Energy Opportunities: From Rooftops to Building Integration. [Online].; 2024. Acceso 20 de Septiembre de 2025. Disponible en: https://www.energy.gov/eere/solar/articles/expanding-solar-energy-opportunities-rooftops-building-integration

8. MITREX. How Integrated Photovoltaics Contribute to LEED Certification. [Online].; 2023. Acceso 20 de Septiembre de 2025. Disponible en: https://www.mitrex.com/blog/how-integrated-photovoltaics-contribute-to-leed-certification

9. de Medeiros Gomes MM, Lopes da Silva Cavalcante RD, Ando Junior OH, Del Pero C, Alves de Lima J, Silva do Lago TG. The Effect of Facade Orientation on the Electrical Performance of a BIPV System: A Case Study in João Pessoa, Brazil. Energies. 2025; 18(829).

https://doi.org/10.3390/en18040829

10. Vera K, Salvatierra J, Lata-García J, Vega N. Analysis of the energy production of photovoltaic facades integrated in BIPV buildings. En: 21st LACCEI International Multi-Conference for Engineering, Education, and Technology: "Leadership in Education and Innovation in Engineering in the Framework of Global Transformations: Integration and Alliances for Integral Development", Hybrid Event, Buenos Aires - Argentina, July 17 - 21, 2023. p. 1 - 7.

https://dx.doi.org/10.18687/LACCEI2023.1.1.1296

11. Sarkar D, Kumar Sadhu P. Critical Comprehensive Performance Analysis of Static BIPV Array Configurations to Reduce Mismatch Loss and Enhance Maximum Power Under Partial Shading. IETE Technical Review. 2023; 40(4).

https://doi.org/10.1080/02564602.2022.2127944

12. Shao C, Migan-Dubois A, Diallo D. Performance of BIPV system under partial shading condition. Solar Energy. 2024; 283.

https://doi.org/10.1016/j.solener.2024.112969

13. Nakazato R, Yokogawa S, Ichikawa H, Ushirokawa T, Takeda T. Compact model for estimating area-level photovoltaic power generation on facade surface using 3D city model and solar radiation simulation. En: 2021 IEEE PES Innovative Smart Grid Technologies - Asia (ISGT Asia)Brisbane; 2021 p. 5.

https://doi.org/10.1109/ISGTAsia49270.2021.9715273

14. Toledo C, Gracia Amillo AM, Bardizza G, Abad J, Urbina A. Evaluation of Solar Radiation Transposition Models for Passive Energy Management and Building Integrated Photovoltaics. Energies. 2020; 13(702).

https://doi.org/10.3390/en13030702

15. Liang H, Shen J, Yip HL, Meng Fang M, Dong L. Unleashing the green potential: Assessing Hong Kong's building solar PV capacity. Applied Energy. 2024; 369.

https://doi.org/10.1016/j.apenergy.2024.123567

16. Ospina-Metaute C, Medina-Garzón L, Betancur E, Marulanda-Bernal J. Study of the optimal orientation of vertical surfaces in different thermal floors in Colombia for solar energy harvesting. Solar Energy. 2022; 239.

https://doi.org/10.1016/j.solener.2022.04.020

17. Chen YJ, Yang YM. Simulation and Analysis of BIPV Solar Panel Configuration on Building Facades. En: IV. International Conference on Electrical, Computer and Energy Technologies (ICECET 2024)Sydney; 2024

https://doi.org/10.1109/ICECET61485.2024.10698325

18. Ismaeil EMH, Sobaih AEE. Evaluating BIPV Façades in a Building Envelope in Hot Districts for Enhancing Sustainable Ranking: A Saudi Arabian Perspective. Buildings. 2023; 13(1110).

https://doi.org/10.3390/buildings13051110

19. Polo J, Martín-Chivelet N, Sanz-Saiz C. BIPV Modeling with Artificial Neural Networks: Towards a BIPV Digital Twin. Energies. 2022; 15(4173).

https://doi.org/10.3390/en15114173

20. Tang H, Chai X, Chen J, Wan Y, Wang Y, Wan W, et al. Assessment of BIPV power generation potential at the city scale based on local climate zones: Combining physical simulation, machine learning and 3D building models. Renewable Energy. 2025; 244.

https://doi.org/10.1016/j.renene.2025.122688

21. Wang M, Zhao X, Li S, Yang Z, Liu K, Wen Z, et al. Analysis of energy performance and load matching characteristics of various building integrated photovoltaic (BIPV) systems in office building. Journal of Building Engineering. 2024; 96.

https://doi.org/10.1016/j.jobe.2024.110313

22. Jing Yang R, Zhao Y, Sureshkumar Jayakumari SD, Schneider A, Prithivi Rajan S, Leloux J, et al. Digitalising BIPV energy simulation: A cross tool investigation. Energy & Buildings. 2024; 318.

https://doi.org/10.1016/j.enbuild.2024.114484

23. Duffie J, Beckman W, Blair N. Solar Engineering of Thermal Processes, Photovoltaics and Wind. 5th ed. Nueva Jersey: Wiley; 2020.

24. Restrepo-Cuestas BJ, Durango-Flórez M, Trejos-Grisales LA, Ramos-Paja CA. Analysis of Electrical Models for Photovoltaic Cells under Uniform and Partial Shading Conditions. Computation. 2022; 10(111).

https://doi.org/10.3390/computation10070111

25. Bastidas-Rodríguez JD, Trejos-Grisales LA, González-Montoya D, Ramos-Paja C, Petrone G, Spagnuolo G. General modeling procedure for photovoltaic arrays. Electric Power Systems Research. 2018; 155.

https://doi.org/10.1016/j.epsr.2017.09.023